Magnetic reversals and mass extinctions

David M. Raup

Department of the Geophysical Sciences, University of Chicago, Chicago, Illinois 60637, USA

Previous analyses of the time distribution of reversals of the Earth's magnetic field have yielded mixed results. Some authors have claimed significant periodicities of order 10^7 yr[1,2] whereas others have reported failure to reject null hypotheses of random spacing at that scale[3–6]. Because of repeated suggestions that field reversal is linked to biological extinction[7–12], further analysis of the magnetic time series is appropriate. I present here the results of a study of the reversal record of the past 165 Myr. A stationary periodicity of 30 Myr emerges (superimposed on the non-stationarities already established by others[5]), which predicts pulses of increased reversal activity centred at 10, 40, 70, ... Myr BP.

The database is the compilation of magnetic reversals for the late Jurassic to present interval (0–165 Myr BP) by Harland *et al.*[13]. These data, constituting the magnetostratigraphical timescale for the best-known part of the reversal record, were culled heavily by Harland *et al.*[13] to eliminate minor excursions and other short-term or local effects and were presented as the time boundaries of 148 magnetic intervals (chrons and subchrons), yielding $148 \times 2 = 296$ reversal events. Figure 1 shows the distribution of these events in geological time, which shows, among other things, the well-known quiet period of the late Cretaceous (83–118 Myr BP), with reversal activity decreasing before and increasing after the quiet period.

In developing the statistical methodology for this analysis, a magnetic reversal is assumed to be an isolated event; thus, it is not important whether the field shifted from normal to reversed or vice versa. The analytical procedure, which follows that of Stothers[14] and Raup and Sepkoski[15], has as a central feature a 'goodness-of-fit' metric applicable to any postulated stationary periodicity. This metric is calculated as follows. For a given trial period (such as 20 Myr), a predicted sequence of events is defined and placed on the timescale in a completely arbitrary phase position (such as −10, 10, 30, 50, ... Myr BP). Then, the fit is assessed as the standard deviation of departures of the observed events from the predicted event closest to each. Thus, in the hypothetical example used here, an event observed at 14 Myr BP would show a departure of +4 Myr from its closest predicted event (10 Myr BP), an observed event at 48 Myr BP would show a departure of −2 (from the 50-Myr BP prediction) and so on. The standard deviation of these departures is a measure-of-fit for a given phase position, which is then shifted by a small increment (to, for example, −9, 11, 31, 51, ... Myr BP) and the standard deviation of departures is recalculated.

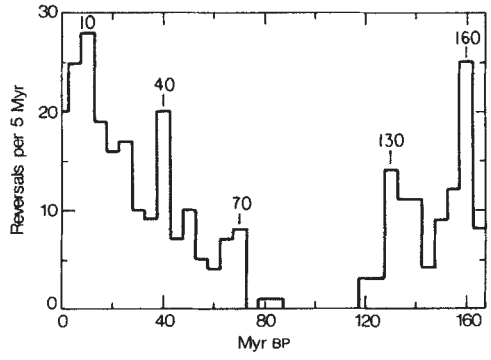

Fig. 1 Frequency of 296 magnetic reversals in 5-Myr intervals (data from ref. 13).

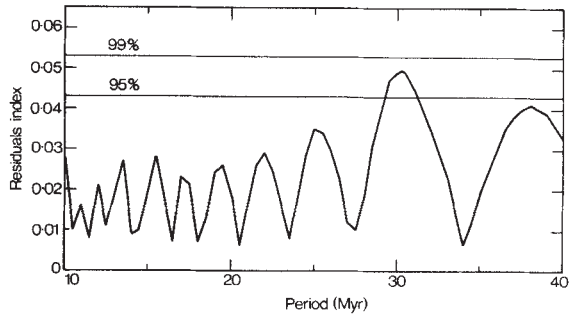

Fig. 2 Spectrum of residuals index ($n = 296$) constructed using the method of Stothers[14]. The residuals index is the measure of goodness of fit of the data to a given period.

This process is repeated for a series of phase increments (totaling at least a full period) and the lowest value of the standard deviation is taken as the goodness-of-fit. We thus have estimates of goodness-of-fit and best-fit position for the trial period. The method is particularly appropriate for time series exhibiting missing or missed data because waiting times between events are never examined explicitly. Also, the method contains no assumption that the frequency behaviour is sinusoidal, contrary to conventional Fourier techniques.

Stothers[14] showed that the standard deviation can be normalized for period length as follows. Residuals index

$$(P\sqrt{(n^2-1)/12n^2} - \sigma)/P$$

where P is the period length, n is the number of observations and σ is the standard deviation of departures (above). With random data, the residuals index is constant over a range of P (but see below).

Given an observed time series, the residuals index may be calculated for a sequence of P values and a spectrum of goodness of fit produced, which is shown in Fig. 2 for the magnetic reversal time series; periods greater than 40 Myr are not included because the residuals index is unstable above $P = 40$ with this particular time series. There are a number of well-defined peaks, but this is not surprising; indeed, random input of the same general character often gives comparable spectra and so it is important to assess the probability that the spectrum is not just the product of chance. Using a bootstrap technique, the real-time series was randomized by scrambling the intervals between successive magnetic reversals; the first and last reversals were used as fixed endpoints and all intervals in between were rearranged by standard Monte Carlo techniques. Each randomized version of the data thus retained most of the fabric of the true series, but the placement of reversals was changed; each had a quiet period

Table 1 Goodness-of-fit and phase for magnetic reversal data

Period (Myr)	Goodness-of-fit: % of simulations with poorer fit than the real data				Phase in best-fit position: age of cycle no. 1		
	0–165	0–83	118–165	(Myr BP)	0–165	0–83	118–165
22	83.6	43.2	96.8		4.49	4.59	4.07
23	45.8	12.2	100.0		0.05	8.59	20.12
24	64.6	20.2	100.0		12.03	8.38	14.13
25	92.2	31.7	100.0		8.35	8.23	8.60
26	84.2	57.5	100.0		7.12	8.91	3.07
27	29.5	75.0	99.9		5.15	7.93	24.27
28	65.1	81.1	99.9		15.03	7.03	19.45
29	98.0	81.7	99.7		12.16	10.62	14.90
30	99.4	82.9	99.6		10.04	10.04	10.05
31	98.9	80.4	99.0		7.80	9.77	5.18
32	96.8	77.5	97.6		5.11	9.20	0.93
33	83.0	74.8	96.5		3.93	8.97	29.04

© 1985 Nature Publishing Group

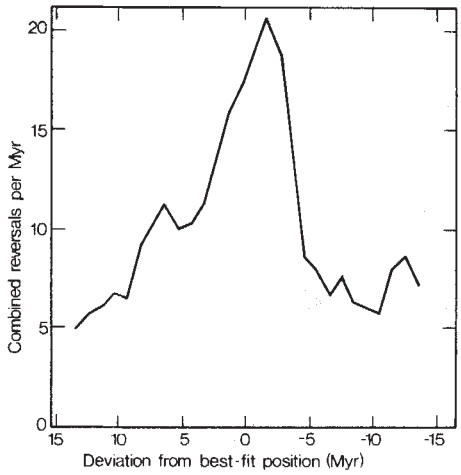

Fig. 3 Composite cycle of magnetic reversal activity plotted as a 3-point moving average. With a 30-Myr period in best-fit position (zero on the horizontal axis), the data from all cycles have been superimposed ($n = 296$).

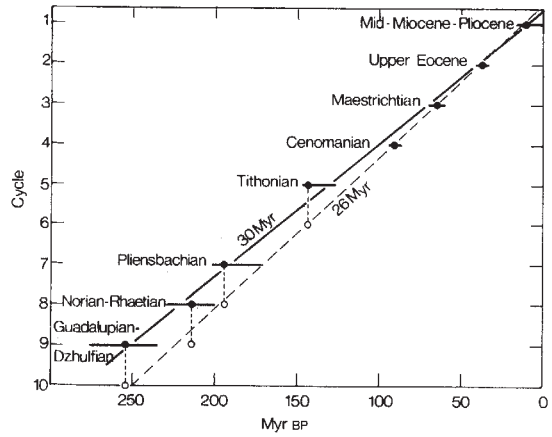

Fig. 4 The distribution by age and cycle number of the eight significant biological extinctions of the last 250 Myr (solid dots). Error bars indicate the maximum possible age spread, including that implied by the several available geological timescales[25]. The solid diagonal corresponds to a 30-Myr period in the best fit position indicated by the magnetic reversal data. If the 26-Myr period is used, the oldest four extinctions must be advanced one cycle each (open circles) and the fit is improved substantially (dashed diagonal).

of the same length, but its position was unpredictable. A spectrum, such as that in Fig. 2, was calculated for each of 200 simulations and the point of highest residuals index for each simulation was recorded. The results are summarized by the two horizontal lines in Fig. 2; 95 and 99%, respectively, of the simulated spectra were contained totally below the designated lines.

The peak corresponding to a period of 30 Myr stands out and is clearly above the 95% line, from which it can be concluded that it is unlikely that the peak is an accident or artefact of the method (Fig. 2). The null hypothesis in this case comes from the above randomization scheme. It is non-Poisson in that the distribution of intervals (waiting times) between events is maintained; only their order has been randomized. Tests with two alternative null hypotheses will be discussed below.

With the 30-Myr peak in Fig. 2 as a starting point, a more detailed investigation of periods in that region was undertaken. For each 1-Myr interval from 22 to 33 Myr, the fit of the real data (measured by the standard deviation of departures) was compared with that of 1,000 simulations of the type used earlier. The results are shown in columns 2 and 5 of Table 1. In column 2, goodness-of-fit is expressed as the percentage of simulations showing a poorer fit (higher standard deviation); the period at 30 Myr is the highest with 99.4%. Column 5 gives the best-fit position expressed as the geological age (in Myr BP) of the most recent pulse of reversal activity and this position for the 30-Myr period is 10.04 Myr BP.

To check these results, the analysis was repeated with non-overlapping segments of the time series, using the Cretaceous quiet period as the demarcation. These results are shown in the remaining columns of Table 1. For the younger segment (0–83 Myr BP), goodness-of-fit values are not as high as for the whole series but the one for 30 Myr is the highest. Also, the best-fit position is identical at 10.04 Myr BP. For the older segment (118–165 Myr BP) all periods show excellent fit, making it difficult to distinguish between them. This is not unreasonable because this segment is only 45 Myr long and contains only two of the events predicted by the complete time series. Note, however, that the best-fit position for the 30-Myr period estimated from this short segment is 10.05 Myr BP, essentially identical to the other estimates for this period. Thus, the analyses of segments can be regarded as confirming a 30-Myr period with a best-fit phase position of 10 Myr BP.

I conclude that the reversal time series probably shows a stationary periodicity predicting elevated reversal activity at 30-Myr intervals beginning at 10 Myr BP. Extrapolating from this conclusion, Fig. 1 shows that the record is dominated by the Cretaceous quiet period with reversal activity increasing in both directions. The 30-Myr periodicity is superimposed on this broader first-order change and can be seen as localized peaks at 10, 40, 70, 130 and 160 Myr BP; the predicted peak at 100 Myr BP is missing because of overall reduction in reversal activity (the quiet period).

I emphasize that a statistical confidence level cannot be assigned to the 30-Myr periodicity. Although the data clearly favour this periodicity over the null hypothesis of random ordering of the same data, an unknown number of stationary and non-stationary models might give as good or a better fit. The 30-Myr stationary model is, nevertheless, the simplest alternative to the random model and seems to be well supported by the data.

Confidence in the 30-Myr periodicity depends on the null hypothesis against which it is tested; it was therefore tested against two other hypotheses. The first is a simple Poisson model where randomization was achieved by 'dropping' 296 points on a 0–165-Myr timescale using uniformly distributed random numbers; the result was identical, within sampling error, to that reported in Table 1. The second variant reproduced the non-stationarities reported by McFadden and Merrill[5]. Once again randomization was achieved by a Poisson method, but in this case the linear decrease in reversal activity before the Cretaceous quiet period and the linear increase after that were used to bias the selection of simulated events. The probabilities used were drawn from linear fits to the actual data following the interpretation of McFadden and Merrill[5]. The result, identical to that reported in Table 1 (99.4% of simulations showing a poorer fit than the real data), confirms further the conclusion that the observed periodicity is superimposed on the larger-scale changes in reversal frequency.

Figure 3 shows the frequency distribution of reversal events in a single composite 30-Myr period. The relatively smooth and symmetrical distribution supports the hypothesis of a 30-Myr period with a best-fit position centred at 10, 40, 70, . . . Myr BP. If other periods or phase positions are used to construct the composite, the distribution breaks down.

These results are in good agreement with other analyses[1,2]. Using Walsh spectrum analysis applied to a much longer series of magnetic reversal data, Negi and Tiwari[1] recognized several periodicities and claimed statistical significance for those at 32 and 285 Myr. Mazaud *et al.*[2], working with the reversal data younger than the Cretaceous quiet period, found a 15-Myr periodicity, which is precisely in phase with the 30-Myr period reported here. Their strongest peaks occurred at 10 and 40 Myr BP and it is not clear (nor especially important) whether the 30-Myr period is a harmonic of the 15-Myr period or vice versa.

© 1985 Nature Publishing Group

What is the relevance of these results to biological extinction? This question involves possible relationships between extinction, comet or asteroid impact and magnetic reversal as well as possible periodicities in all three. The link between extinction and magnetic reversal is supported by some studies[7-12] but challenged by others[16-17]; that between extinction and impact is more nearly established because of the iridium and/or other evidence for impact at four separate extinction times—late Eocene[18-19], terminal Cretaceous[20-21], terminal Permian[22] and late Devonian[23]. Further, the suggestion that extinctions and impact events are both periodic and in phase[12,24-26] strengthens the case for causal linkage. A proposed link between large-body impact and magnetic reversal is more tenuous, but is supported by some evidence, specifically the temporal coincidence of magnetic reversals with three of the four well-dated tectite-strewn fields[27]. It is thus not impossible that at least some reversals are caused by comet or asteroid impact and it is in this context that the relationship between periodic intensification of reversal activity and periodic extinction becomes important.

For the most recent several cycles, the fit between extinctions and reversal intensity is reasonable in view of the extinctions at 11.3, 38 and 65 Myr BP[25] and the magnetic reversal peaks at 10, 40 and 70 Myr BP. But because the most probable periodicity for extinctions is 26 Myr[15,25], the two systems move out of phase going backwards in time. This is illustrated in Fig. 4, which shows an attempt to fit the 30-Myr periodicity to the eight significant extinctions of the past 250 Myr and shows also the 26-Myr fit to the same extinction points. Except for the first three events, the discrepancy between the two periods is clearly non-trivial.

The discrepancy can mean either there are independent periodicities operating with no causal connection or that the statistical uncertainty of the analyses is large enough to accommodate a single period somewhere in the 26-30-Myr range. The situation is complicated further by the fact that Rampino and Stothers[12] re-analysed the extinction data and found a best-fit period of 30 ± 1 Myr, with phase position at 10 ± 7-Myr BP. They used a regression method that assumes that all cycles are present in the data, although they noted that removing this restriction restores the 26-Myr period of Raup and Sepkoski[15,25].

The discrepancies in analytical results mean that no unequivocal conclusion can be drawn; however, there is a possibility that biological extinction, magnetic reversal and large-body impact are linked.

I thank M. R. Rampino, J. J. Sepkoski Jr, S. Stigler and R. B. Stothers for discussions and also G. E. Boyajian for literature search and for help with the analysis of the magnetic data. The work was supported by NASA grant NAG 2-237.

Received 21 September 1984; accepted 22 January 1985.

1. Negi, J. G. & Tiwari, R. K. *Geophys. Res. Lett.* **10**, 713-716 (1983).
2. Mazaud, A., Laj, C., de Sèze, L. & Verosub, K. L. *Nature* **304**, 328-330 (1984).
3. Phillips, J. D. & Cox, A. *Geophys. J. R. astr. Soc.* **45**, 19-33 (1976).
4. Cox, A. *Phys. Earth Planet. Interiors* **24**, 178-190 (1981).
5. McFadden, P. L. & Merrill, R. T. *J. geophys. Res.* **89**, 3354-3362 (1984).
6. McFadden, P. L. *Nature* **311**, 396 (1984).
7. Uffen, R. J. *Nature* **198**, 143-144 (1963).
8. Simpson, J. F. *Bull. geol. Soc. Am.* **77**, 197-204 (1966).
9. Hatfield, C. B. & Camp, C. J. *Bull. geol. Soc. Am.* **81**, 911-914 (1970).
10. Hays, J. D. *Bull. geol. Soc. Am.* **82**, 2433-2447 (1971).
11. Crain, I. K. *Bull. geol. Soc. Am.* **82**, 2603-2606 (1971).
12. Rampino, M. R. & Stothers, R. B. *Nature* **308**, 709-712 (1984).
13. Harland, W. B. *et al. A Geologic Time Scale* (Cambridge University Press, 1982).
14. Stothers, R. B. *Astr. Astrophys.* **77**, 121-127 (1979).
15. Raup, D. M. & Sepkoski, J. J. *Proc. natn. Acad. Sci. U.S.A.* **81**, 801-805 (1984).
16. Thomson, K. S. in *Patterns of Evolution* (ed. Hallam, A.) 377-404 (Elsevier, Amsterdam, 1977).
17. Plotnick, R. E. *Geology* **8**, 578-581 (1980).
18. Ganapathy, R. *Science* **216**, 885-886 (1982).
19. Alvarez, W., Asaro, F., Michel, H. V. & Alvarez, L. W. *Science* **216**, 886-888 (1982).
20. Alvarez, L. W., Alvarez, W., Asaro, F. & Michel, H. V. *Science* **208**, 1095-1108 (1980).
21. Alvarez, W. *et al. Science* **223**, 1135-1141 (1984).
22. Sun, Y. *et al.* in *Developments in Geoscience*, 235-245 (Academia Sinica, Science Press, Beijing, 1984).
23. Playford, P. E., McLaren, D. J., Orth, C. J., Gilmore, J. S. & Goodfellow, W. D. *Science* **226**, 437-439 (1984).
24. Alvarez, W. & Muller, R. A. *Nature* **308**, 718-720 (1984).
25. Sepkoski, J. J. & Raup, D. M. in *Dynamics of Extinction* (ed. Elliott, D.) (Wiley, New York, in the press).
26. Rampino, M. R. & Stothers, R. B. *Science* **226**, 1427-1431 (1984).
27. Glass, B. P., Swincki, M. B. & Zwart, P. A. *Proc. 10th Lunar Planet. Sci. Conf.* 2535-2545 (1979).

Lead isotope differences between whole-rock and phenocrysts in recent lavas from southern Italy

M. Cortini* & P. W. C. van Calsteren†

* Istituto di Geologia & Geofisica, University of Naples, 80138 Naples, Italy
† Department of Earth Sciences, Open University, Milton Keynes MK7 6AA, UK

In southern Italy, there are several active volcanoes which occur in diverse geotectonic settings. Isotope determinations on coexisting minerals and whole-rocks from zero-age lavas from Vesuvius, Etna and Stromboli reveal an isotope equilibrium for Sr isotopes[1] but not for Th (ref. 2). Analyses for Pb in the same samples also reveal differences in isotope composition, and in all cases the phenocrysts are less radiogenic than the whole-rocks. We argue here that the Pb and Th isotope composition of the magmas changed during and after fractional crystallization, possibly by crustal assimilation or by addition of mantle-derived fluids and that whole-rock Pb isotope data are not representative of the magma sources.

Stromboli forms part of the Aeolian island arc, probably along a destructive margin between the European and African plates. It is characterized by virtually uninterrupted eruption of leucite tephrites and basaltic andesites belonging to the high-K-calc-alkaline series. Model calculations based on trace elements indicate an origin by partial melting of a parent material inhomogenously enriched by a Th/light rare-earth element/P-rich metasomatic fluid, probably derived from the subducting plate[3].

Etna is a large alkali basalt volcano, with minor early tholeiitic lavas, producing mainly hawaiites and mugearites. Its geochemistry is largely consistent with its within-plate setting but a minor modification of its source by subduction-derived phases is likely[3].

Vesuvius is best known for its explosive-effusive eruptions of high-K trachytes and leucite tephrites; they probably derive from a comparatively recently enriched mantle source, by analogy with nearby Roccamonfina[4]. Fractional crystallization and cumulus formation took place in various magma chambers at different levels in the crust; the incorporation of limestone fragments, high in the crust, had little effect on the volcanic rocks.

Table 1 shows the results of our analyses of the Pb isotope composition of whole-rock and mineral separates of lavas and ejected cumulates of well-studied samples. Separated minerals are either phenocrysts, considered to have crystallized from the coexisting magma, or biotite separated from nodules which have been interpreted as cumulates[5].

Pb was separated using a 0.1-ml AG 1×8 ion-exchange column, eluted with 1M HBr and stripped with 2 ml H_2O. Pb was loaded on a Re filament with phosphoric acid and silica gel. Isotope ratios were measured using our software on a VG54E mass spectrometer. The NBS 981 standard was run in the same conditions and from the collated results a bias factor of 1.00047 AMU^{-1} was calculated. Measured results were corrected using this factor to minimize the effects of instrumental mass fractionation. The total procedure blank is <2 ng; sample weights were adjusted to contain an estimated 1 μg Pb.

Our data for the Vesuvius 1944 lava are in agreement with Vollmer and Hawkesworth[6], while those from the Etna lavas compare well with the data of Carter and Civetta[7]. Reproducibility may be estimated from the two duplicate whole-rock analyses.

There are no significant differences in Sr isotope ratios (Table 1) between phenocrysts and their whole-rocks, indicating that phenocrysts are indeed co-magmatic. Differences in Sr isotopes between Vesuvius samples from different magma batches can be explained by mixing two endmembers with very similar major-element, but different isotope, compositions[1].

© 1985 Nature Publishing Group